Toxicity Measurement of Halogeno-benzene against Vibrio Qinghaiensis (Q67) and Their 2D,3D-QSAR Study①

GE Zhi-Gang② SUN Ping
LIU Hui TAN Jun LIU Hong-Xia
(*School of Biological and Chemical Engineering, Jiaxing University, Zhejiang* 314001*, China*)

ABSTRACT Toxicities ($-\lg EC_{50}$) of 16 halogeno-benzenes against vibrio qinghaiensis (Q67) were measured systematically, and their 2D-QSAR model ($R^2 = 0.875$, $q^2 = 0.821$) was established, which included two parameters: averaged polarizability (α) and total energy (*TE*). The proposed model indicated that the toxicities of this kind of compounds were proportionate to α, i.e., their toxicities were relative to the molecular volume. Furthermore, 3D-QSAR model ($R^2 = 0.929$, $q^2 = 0.712$) of $-\lg EC_{50}$ was proposed by using comparative molecular force field (CoMFA) based on the molecular simulation. To our interest, 3D-QSAR model suggested that the hydrophobicity of substituents was the dominating factor for the toxicities, the electrostatic effect was the secondly important, and the steric field gave the least contribution. Comparably, the prediction ability of the 3D-QSAR model is slightly more advantageous than that of 2D-QSAR, and they can be used complementally in the toxicity description of this kind of compounds.

Keywords: halogeno-benzenes, vibrio qinghaiensis (Q67), quantitative structure-activity relationship (QSAR), density functional theory (DFT), CoMSIA

1 INTRODUCTION

As a kind of widely used organic compounds, halogeno-benzenes are also pollutants, whose toxicities have captured attention from all over the world. So far, their properties and toxicities have been studied extensively. For example, Bahadur *et al*.[1] disclosed the relationship between octanol/water distribution coefficient and temperature of chloro-benzenes; Shiu *et al*.[2] investigated the relationship between solubility in water and temperature of chlorobenzenes; Lin *et al*.[3] predicted the toxicities of halogeno-benzene mixtures with distribution coefficient; Finizio *et al*.[4] estimated the relationship between octanol/water distribution coefficient and temperature of chloro-benzenes using reverse high performance liquid chromatography (HPLC) method; Kong *et al*.[5] studied the structures of four halogeno-benzenes and their biological toxicities against selenastrum capricornutum; Liu *et al*.[6] revealed the inhibiting and DNA destroying effects of chloro-benzenes in pollution soil; Chaufan *et al*.[7] investigated the toxicity of hexachloro-benzene and its transferring rule from Chlorella kessleri microalgae to Chasmagnathus granulatus crab.

At present, the toxicity evaluation of environment pollutants is generally executed by using aquatic indicator organisms, including nematode, photobacterium phosphoreum, daphnia magna, algae (for example, green algae), macrophytic algae, fish,

Received 30 April 2010, accepted 12 November 2010
① This work was supported by the Analysis Science and Technology Project of Zhejiang Province (2009F70007)
② Corresponding author. Tel: 13857368434, Fax: 0573-83641881, E-mail: squirrel81@126.com

todpole, juvenile prawn and fluke. Among them, photobacterium phosphoreum toxicity measurement is widely adopted due to its convenience, high sensitivity and efficiency. Furthermore, toxicities against photobacterium phosphoreum exhibit some correlation with those against other organisms[8, 9]. Therefore, this method is universally accepted in the screening of toxic chemicals and their environmental risk assessment, which can provide elemental data for studying their toxicities against other organisms. As a testing species of freshwater photobacteria toxicity, vibrio qinghaiensis (Q67) exhibits many advantages including lower Na^+ concentration, moderate temperature and wider pH range compared with marine photobacteria.

Quantitative structure-activity relationship (QSAR) is an important tool used in structure/activity prediction and action mechanism description of toxic compounds[10, 11]. In the environmental science field, QSAR methods include traditional 2D-QSAR and 3D-QSAR, and the former has been well established and widely used in ecotoxicology[12~15]. However, 3D-QSAR is a hot studying field in QSAR and has been applied in medicine field, but it is still in its infancy in environmental application[16, 17]. In this work, toxicity data (EC_{50} (mol/L)) of 16 halogenobenzenes (including 5 chloro-benzenes, 8 fluobenzens and 3 bromobenzenes) against vibrio qinghaiensis (Q67) were measured. In addition, structural and thermodynamic parameters of halogenobenzens were calculated at the 6-311G** level with DFT method in Gaussian 03 program[18], upon which the 2D-QSAR model between $-\lg EC_{50}$ and structural parameters was proposed, and furthermore, the 3D-QSAR model using comparative molecular force field (CoMFA) was established. Finally, these two models were compared in detail.

2 EXPERIMENTAL

2.1 Apparatus

The following apparatuses were used in this work: water toxicity rapid detector (BHP9511, (Beijing Hamamatsu Photonics Co., Ltd), constant temperature oscillating incubator (HNY-2000B, Tianjin Honour Instrumont Co., Ltd), automatic autoclaving pot (SA-300VF-F-A501, Sturdy Industrial Co., Ltd).

All the chemicals were analytically pure and listed in Table 1.

Table 1. Compounds and Their Quantum Chemical Parameters Based on the B3LYP/6-311G Calculation**

No.	Molecule	V_m Å^3	E_{HOMO} eV	E_{LUMO} eV	*TE* Hartree	S^o J·mol^{-1}·K^{-1}	μ Debye	α 10^{-30}esu
1	Chlorobenzene	143.97	–0.2557	–0.0255	–691.9306	318.94	1.9731	70.74
2	1,3-Dichlorobenzene	163.88	–0.2633	–0.0391	–1151.5508	349.06	1.8416	83.01
3	4-Chloro-3-fluorotoluene	171.28	–0.2511	–0.0326	–830.5184	386.26	3.1595	84.57
4	1,2,4-Trichlorobenzene	181.75	–0.2630	–0.0499	–1611.1660	377.86	1.4175	95.22
5	1,2-Dichlorobenzene	161.98	–0.2606	–0.0367	–1151.5469	347.72	2.8191	81.87
6	Fluorobenzene	123.30	–0.2547	–0.0224	–331.5730	307.31	1.5191	59.14
7	1,2-Difluorobenzene	126.76	–0.2586	–0.0273	–430.8300	326.00	2.5192	59.28
8	1,3-Difluorobenzene	122.65	–0.2610	–0.0286	–430.8363	325.69	1.5007	59.17
9	1,4-Difluorobenzene	120.79	–0.2536	–0.0352	–430.8353	325.90	0.0002	59.15
10	1,2,4-Trifluorobenzene	133.06	–0.2602	–0.0384	–530.0914	344.45	1.4140	59.39
11	1,3,5-Trifluorobenzene	130.03	–0.2732	–0.0277	–530.0983	344.10	0.0005	59.35
12	1,2,4,5-Tetrafluorobenzene	135.84	–0.2631	–0.0451	–629.3457	363.33	0.0009	59.59
13	1-Fluoro-4-nitrobenzene	150.37	–0.2888	–0.1002	–536.1283	367.67	3.1380	75.58
14	Bromobenzene	153.23	–0.2513	–0.0251	–2805.8510	330.90	1.8524	76.91
15	1,2-Dibromobenzene	181.54	–0.2550	–0.0378	–5379.3875	371.08	2.4848	93.85
16	1,3-Dibromobenzene	179.98	–0.2576	–0.0386	–5379.3920	372.89	1.6884	95.79

2. 2 Experimental strain

Freshwater photobacteria-vibrio qinghaiensis (Q67)(Vibrio-qinghaiensis sp. –Q67) was provided by biological department of East-China Normal University and the culture of strain was carried out according to literature[19]: ampoule bottle containing freeze-dried powder was kept in iceberg at 4 ℃ for 10～15 min, and the ampoule bottle was cut on a superclean bench. 100 mL 0.8% NaCl solution having been disinfected was spotted on the culture dish. The stain was moved to the solution with inoculating loop and kept in a constant temperature incubator at 22 ℃ for 24 h. Single strain was inoculated on the inclined medium and cultured at 22 ℃ for 24 h. Afterwards, it was inoculated on the inclined medium again and kept in iceberg at 4 ℃. The cultured strain was moved to 15 mL liquid culture medium and oscillated 22 ℃ for 16～24 h.

2. 3 Toxicity measurement

The test compounds with certain amount were dissolved in distilled water and used to determine the concentration range (photo-inhibition rate was set at about 50%). The detailed operation method is: if the concentration of mother solution is a, the concentration range in the pre-experiment can be set as 0.1a, 0.01a, 0.001a and 0.0001a. According to the results of pre-experiments, five concentration gradients were given around the 50% photo-inhibition rate, and three parallel samples were used at each concentration. During the measurement, 2 mL solution was added into the colorimetric tube using distilled water as blank. 0.5 mL diluted bacterial liquid was moved into the colorimetric tube quickly and shaken up and down for 10 times. 15 min later, the luminous intensity was recorded with BHP9511 biological toxicity measurement apparatus, and EC_{50} (mol/L) was calculated as the concentration at the photo-inhibition rate of 50% using linear interpolation method. Two parallel experiments were carried out for each concentration. Their standard error was lower than 10%, as can be seen in Table 2.

Table 2. Experimental, Predicted –lgEC_{50} Values and Their Difference of Halogeno-benzenes

No*.	Exp.	Eq.(3)		Eq.(4)		CoMSIA	
		Pred.	Res.	Pred.	Res.	Pred.	Res.
1	3.434	2.828	–0.606	2.737	–0.697	3.526	0.092
2	3.542	3.297	–0.245	3.216	–0.326	4.030	0.488
3	2.889	3.202	–0.313	3.114	0.225	2.984	0.095
4	3.875	3.765	–0.110	3.695	–0.180	3.741	–0.134
5	3.264	3.271	0.007	3.190	–0.074	3.751	0.487
6	2.592	2.414	–0.178	2.315	–0.277	2.551	–0.041
7	2.297	2.458	0.161	2.361	0.064	2.196	–0.101
8	3.059	2.455	–0.604	2.358	–0.701	2.525	–0.534
9	2.362	2.455	0.093	2.358	–0.004	2.315	–0.047
10	2.591	2.501	–0.090	2.406	–0.185	2.263	–0.328
11	2.211	2.500	0.289	2.405	0.194	2.196	–0.015
12	2.337	2.546	0.209	2.453	0.116	2.080	–0.257
13	2.438	2.876	0.438	2.781	0.343	2.416	–0.022
14	3.115	3.830	0.715	3.787	0.672	3.171	0.056
15	5.595	5.267	–0.328	5.284	–0.311	4.978	–0.617
16	5.259	5.312	0.053	5.328	0.069	5.213	–0.046

*The name of compounds is the same with those in Table 1.

3 CALCULATION METHOD AND FOUNDATION OF MODELS

3. 1 Parameter calculation and theoretical base of 2D-QSAR

The full optimization on molecular structures was carried out with B3LYP/6-311G** basis set. Frequency analysis suggested that no imaginary frequency was observed, so the geometries were all local minimal on the potential surfaces. Keyword

"Volume" was used to denote the molecular volume (V_m). Structural parameters include: dipole (μ), energy of the highest occupied molecular orbital (E_{HOMO}), energy of the lowest unoccupied molecular orbital (E_{LUMO}), the most negative atomic charge (q^-), the most positive H atom charge (qH$^+$), molecular volume (V_m) and molecular averaged polarizability (α). Thermodynamic parameters include: total energy (*TE*), zero point energy (*ZPE*), enthalpy (H^θ), free energy (G^θ), correction value of thermal energy (E_{th}), molar heat capacity at constant volume (C_V^θ) and entropy (S^θ). Some of the quantum chemical parameters are listed in Table 1.

Based on the experimental data of –lgEC_{50}, 2D-QSAR model was established using quantum chemical parameters as theoretical descriptors with SPSS 12.0 for Windows program.

3. 2 CoMSIA model

3D-QSAR model was established with classic comparative molecular force field (CoMFA). CoMFA analysis was executed with SYBYL 7.3 program: Tripos standard field was adopted, the hold value of electrostatic and steric fields was set at 30 kcal·mol^{-1}; the size and distribution of electrostatic and steric fields were calculated by using sp^3 hybrid C^+ as probe at an interval of 2.0 Å. Other values were default.

Molecular structures of all compounds were optimized by Tripos standard molecular force field with energy cut-off of 0.05 kcal·mol^{-1}·Å^{-1}. The atomic net charges were calculated with Gasteriger-Hückel method. All the compounds contain benzene ring which is thus used as the folding skeleton. The 15th compound (1,2-dibromobenzene) with the highest toxicity was set as the folding template.

The statistic analysis was executed with the partial least-squares regressive analysis (PLS), and LOO (leave-one-out) method was utilized to determine the optimal principal component number *n* and cross-validation related coefficient (q^2), and then the CoMSIA model was verified with the non-cross-validation. The stability of proposed model was validated by the cross-validation related coefficient (q^2), normal related coefficient (R^2), standard error and F-test value (F)[20].

4 RESULTS AND DISCUSSION

4. 1 Dependent equation of –lgEC_{50} (halogenobenzene against vibrio qinghaiensis (Q67))

Based on the multiple linear regression on experimental and theoretical data (Table 3) of –lgEC_{50}, the dependent equation was established using calculated structural and thermodynamic parameters as theoretical descriptors with SPSS 12.0 for Windows program:

$$-\lg EC_{50} = 0.919 + 0.023\alpha - 0.407TE/1000 \quad (1)$$

$$R^2 = 0.875,\ SE = 0.384,\ q^2 = 0.821,\ F = 45.4$$

Here, R^2, *SE*, q^2 and *F* are related coefficient, standard error, cross-validation related coefficient and F-test value, respectively.

As indicated by equation (1), molecular averaged polarizability (α) and total energy (*TE*) appear in the equation. R^2 (0.875), *SE* (0.384), q^2 (0.821) and *F* (45.4) suggest good stability and prediction ability of equation (1). The predicted values with equation (1) are given in Table 2, among which compound 14 (bromobenzene) exhibits the largest residual error of 0.715.

In order to validate the stability of model (I), 16 compounds in Table 1 are divided into two groups (training set and test set): the former three compounds in every four are merged into the training set, and the rest 4 compounds are treated as the test set, i.e., the 4th, 8th, 12th and 16th compounds are in the test set. Multiple linear regression on the training set gives equation (2):

$$-\lg EC_{50} = 0.811 + 0.024\alpha - 0.425TE/1000 \quad (2)$$

$$R^2 = 0.846,\ SE = 0.402,\ q^2 = 0.818,\ F = 24.787$$

In equation (2), R^2 = 0.846, *SE* = 0.402, q^2 = 0.818 and *F* = 24.787. All the above factors are close to those of equation (1). The predicted values of the training and test sets with equation (2) are listed in Table 2, which illustrates the good prediction ability of equation (2) on the 4 compounds in the test set. Among them, compound 8 (1,3-difluorobenzene) exhibits the largest residual error of –0.701. The

other predicted values are close to the experimental data, suggesting good stability and prediction ability of this 2D-QSAR model.

As revealed by equations (1) and (2), the toxicities of this series of compounds are mainly dominated by molecular polarizability (α) and total energy (*TE*). In detail, toxicities are proportional to α. We can explain it as follows: α indicates the dipole amount induced by adjacent molecule with permanent or temporary dipole, so it expresses the volume property. In other words, the volume will increase with the augment of α. In the mean time, α also expresses the deformability of molecular charge. The higher α suggests the more deformability of molecular charge. Consequently, the molecule will enter into the organism phase more easily compared with its entrance into water phase, and ultimately, it will exhibit higher toxicity. On the other hand, toxicities are inversely correlated to *TE*, because *TE* reflects the molecular total energy. The more negative the *TE* is, the higher toxicity the compound will possess.

4. 2 Evaluation on equation (1)

The correlation degree of all variables in equation (1) was evaluated by variance inflation factors (*VIF*). *VIF* was defined as: $VIF = 1/(1 - r^2)$, where r is the multiple regression correlation coefficient between one variable and the others. If $VIF = 1.0$, no correlation among the variables will appear. $VIF = 1.0 \sim 5.0$ suggests an acceptable correlation. $VIF > 10$ indicates that the regression equation is unstable and re-check seems necessary. Self-correlation coefficients (r^2) of α and *TE*, *VIF*, standard regression coefficients (*SR*) and *t*-values are given in Table 3.

Table 3. Self-correlation Coefficients (r^2), Variance Inflation Factors (*VIF*), Standard Regression Coefficients (*SR*) and *F*-Values of Equation (3)

Variable	r^2	*VIF*	*SR*	$t(t_{\alpha/2} = 2.120)$, $\alpha = 0.05$
α	0.529	2.124	0.326	2.279
TE	0.529	2.124	–0.671	–4.687

As revealed by Table 3, correlation coefficients (r^2) of two dependent variables in equation (1) are both 0.529, and *VIF* are 2.124. These two coefficients are both smaller than 5.0, suggesting a negligible correlation among each variable and good statistic significance/stability of the model. In the confidence range of 95%, standard *t*-value ($t_{\alpha/2}$) is 2.120, and *t*-values of α and *TE* are respectively 2.279 and –4.687, which are both larger than the standard *t*-value ($t_{\alpha/2}$). This further verifies the stability of equation (1). Standard regression coefficients (*SR*) of two variables in equation (1) are listed in Table 3. Clearly, *SR* of *TE* (–0.671) is larger than that of α (0.326). Therefore, conclusion could be drawn that the effect of *TE* on toxicity will be more notable than that of α.

4. 3 3D-QSAR model

The folding diagrams of 16 compounds are given in Fig. 1. As expected, all the molecules can be well folded.

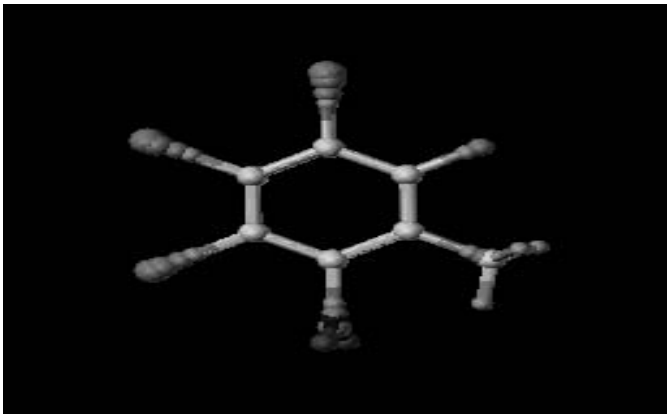

Fig. 1. Molecular folding map of the halogeno-benzenes

During the foundation of 3D-QSAR model with CoMFA method, the test set is the same with that in the 2D-QSAR model (the 4th, 8th, 12th and 16th compounds are in the test set). PLS analysis is carried out on the training set and the results are given in Table 4.

Table 4. Statistic Parameters Based on the CoMSIA Model of –lgEC_{50}

	Model	*n*	q^2	R^2	*SE*	*F*	S	E	H
–lgEC_{50}	CoMSIA	3	0.712	0.929	0.334	39.168	0.120	0.366	0.514

S, E and H are the steric, electrostatic and hydrophobic fields

As given by Table 6, the optimal principal component number *n of* CoMFA model is 3, R^2 is 0.929, *SE* is 0.334 and *F* is 39.618. Specially, the cross-validation related coefficient q^2 is 0.712 (> 0.5), suggesting a good prediction ability of this model. The above data illustrate that CoMFA model possesses good stability and prediction ability. The predicted values and the differences of 16 compounds are listed in Table 3. Among 16 com- pounds, compound 15 (1,2-dibromobenzene) exhi-bits the largest difference of –0.617. The predicted values of other compounds are close to the experimental data, indicating the good predicting ability of CoMFA model. In view of the field energy con-tribution, hydrophobic field gives the contribution of 0.514, electrostatic field exhibits 0.204 contribution, and the least is the steric field (0.796). Judging from this, the toxicities of this kind of compounds are mainly affected by the hydrophobic properties of substituents. Electrostatic and steric fields play the secon-dly and thirdly important roles. Hydrophobicity is closely relative to the molecular volume. In the present work, the introduction of "-Br" group at the same position will lead to larger volume than that of "-Cl" or "-F" groups, but their hydrophobicity will decrease. In other words, for halogenobenzenes, larger molecular volume will result in stronger hydrophobicity, and consequently, the worse water solubility. In the 2D-QSAR model, molecular polarizability α can affect the toxicity greatly, and it is also relative to the molecular volume. Therefore, complementary results can be obtained with 2D-QSAR and CoMSIA model.

4. 4 3D equipotential map of the CoMFA model

The 3D equipotential map of CoMFA model is given in Fig. 2 (1,2-dibromobenzene is set as an example). Fig. 2(a) is the distribution diagram of steric field. The yellow zone denotes that the introduction of substituted group with smaller volume will lead to higher toxicity. Fig. 2(b) is the distribution diagram of electrostatic field, in which the blue zone indicates that the introduction of more electronegative substituted groups will lead to lower toxicity. Finally, Fig. 2(c) is the distribution diagram of hydrophobic field, where the white zone presents that the introduction of substituted group with stronger hydrophobicity will result in higher toxicity.

As revealed by Fig. 2, in the electrostatic field, the ortho-position is covered by the blue color, suggesting that the introduction of more electronegative substituted groups in this zone will lead to lower toxicities. As is known to all, the electronegative orders of halogen atoms are: -F > -Cl > -Br, so the toxicity order is: 1,2-difluorobenzene < 1,2-dichlorobenzene < 1,2-dibromobenzene. In the hydrophobic field, the zone around benzene is covered by white color, so the introduction of substituted group with stronger hydrophobicity leads to higher toxicity. The atomic volume order is: Br > Cl > F, and Br exhibits the strongest hydrophobicity. Thereby, in this zone, the introduction of Br will give rise to higher toxicity than that of Cl- and F-introduction. The 3D equipotential map can disclose the toxic mechanism clearly, which is the same with the experimental data.

4. 5 Comparison between the 2D-QSAR and 3D-QSAR models

The comparison is conducted from two viewpoints of toxic mechanism and prediction ability. 2D-QSAR model suggests that both the molecular

polarizability α and the total energy *TE* can affect the toxicity greatly. Toxicities are proportional to α. In detail, α expresses the volume property. The volume will increase with the augment of α. At the mean time, α also expresses the deformability of molecular charge; the higher α indicates the more deformability of molecular charge; consequently, the molecule will enter into the organism phase more easily compared with its entrance into the water phase; and ultimately, it will exhibit higher toxicity. Judging from 3D-QSAR model, the toxicities are mainly affected by the hydrophobic properties of substitutents. For halogeno-benzenes, hydrophobicity is closely relative to the molecular volume. Comparably, the introduction of "-Br" group with larger volume will lead to higher hydrophobicity, and consequently, worse water solubility and higher toxicity. Thus, complementary results can be obtained with 2D-QSAR and CoMSIA models, which can provide theoretical guide to the application of QSAR in the environmental chemical field.

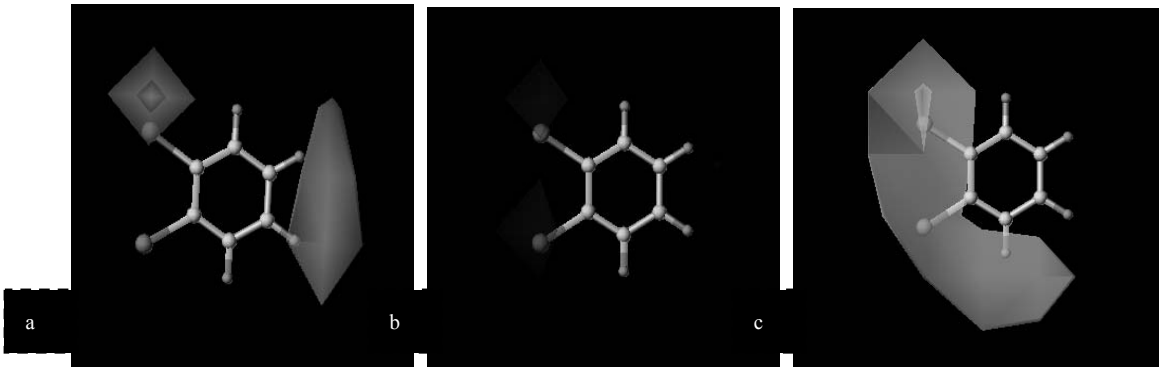

Fig. 2. 3-D Equipotential map of the electrostatic field (a), steric field (b) and hydrophobic field(c) with CoMFA model

Fig. 3 illustrates the predicted difference between 2D and CoMSIA models, from which the predicted accuracy of two models can be seen visually. In equation (3), compound 14 (bromobenzene) exhibits the largest error of 0.715. The absolute errors of the rest 15 compounds are all smaller than 0.600. The averaged absolute error of 16 compounds is 0.277. In the CoMSIA model, compound 15(1,2-dibromo-ben-zene) presents the largest error of –0.617, and the averaged absolute error of 16 compounds is 0.210. Setting relative error of 15% as boundary, in equation (1), the number of compounds with relative error smaller than 15% is 12, but in the CoMSIA model, this number is as high as 15. Therefore, generally, the CoMSIA model has stronger prediction ability than 2D-QSAR.

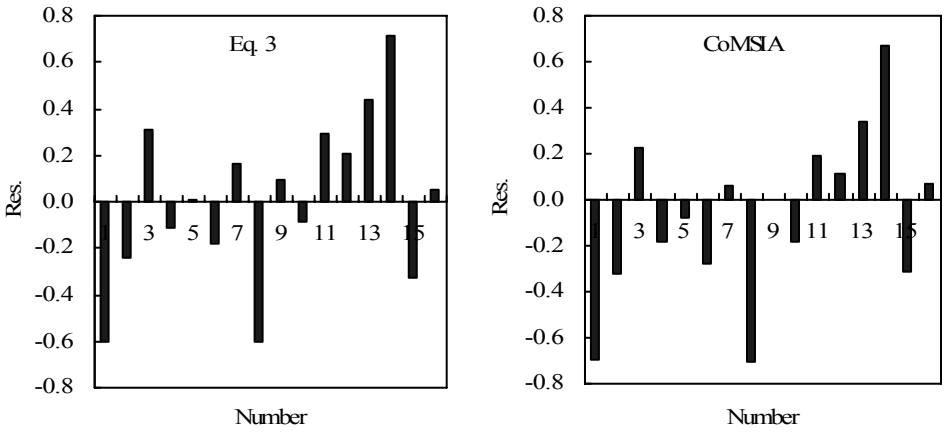

Fig. 3. Difference column diagram of the predicted values with two models

5 CONCLUSION

The quantum chemical parameters of part halogeno-benzenes were calculated at the B3LYP/6-311G** level, based on which the 2D-QSAR model of $-\lg EC_{50}$ was proposed. To our interest, this model exhibits good stability and prediction ability judging from the values of R^2 (0.875), *SE* (0.384), q^2 (0.821) and *F*-value (45.4). The model analysis suggested that the toxicities of this kind of compounds were mainly affected by molecular polarizability (α) and total energy (*TE*), where the toxicities were proportional to α. In the mean time, the 3D-QSAR model was proposed by using comparative molecular force field (CoMFA) based on the molecular simulation, which also exhibits good stability and prediction ability. 3D equipotential map illustrates the effect of different substituents on their toxicity. In detail, hydrophobicity of substituents was the dominating factor for the toxicities, the electrostatic effect was the secondly important, and the steric field gave the least contribution. Thereby, complementary results can be obtained with 2D-QSAR and CoMSIA models. Comparably, the prediction ability of 3D-QSAR model was slightly more advantageous than that of 2D-QSAR. They can be used complementally in the toxicity description of this kind of compounds. This work will provide further theoretical guide for the studying of biological toxic mechanism of halogeno-benzenes.

REFERENCES

（1） Bahadur, N. P.; Shiu, W. Y.; Boocock, D. G. B.; Mackay, D. *J. Chem. Eng. Data* **1997**, 42, 685–688.

（2） Shiu, W. Y.; Wania, F.; Hung, H.; Mackay, D. *J. Chem. Eng. Data* **1997**, 42, 293–297.

（3） Lin, Z. F.; Shi, P.; Gao, S. X.; Wang, L. S.; Yu, H. X. *Water Res.* **2003**, 37, 2223–2227.

（4） Finizio, A.; Guardo, A. D. *Chemosphere* **2001**, 45, 1063–1070.

（5） Kong, F. X.; Hu, W.; Liu, Y. *Environ. Exp. Bot.* **1998**, 40, 105–111.

（6） Liu, W.; Yang, Y. S.; Li, P.; Zhou, Q.; Sun, T. *Chemosphere* **2004**, 57, 101–106.

（7） Chaufan, G.; Juárez, Á.; Basack, S.; Ithuralde, E.; Sabatini, S. E.; Genovese, G.; Oneto, M. L.; Kesten, E. *Toxicology* **2006**, 227, 262–270.

（8） Zhao, Y. H.; He, Y. B.; Wang, L. S. *Toxicol. Environ. Chem.* **1995**, 51, 191–195.

（9） Zhao, Y. H.; Wang, L. S.; Gao, H.; Zhang, Z. *Chemosphere* **1993**, 26, 1971–1979.

（10） Hansch, C.; Muir, R. M.; Fujita, T. *J. Am. Chem. Soc.* **1963**, 85, 2817–2824.

（11） Hansch, C.; Fujita, T. *J. Am. Chem. Soc.***1964**, 86, 1616–1626.

（12） Li, X. J.; Shan, G.; Liu, H.; Wang, Z. Y. *Chinese J. Struct. Chem.* **2009**, 28, 1236–1241.

（13） Liu, H.; Sun, P.; Chen, J. T.; Wang, Z. Y. *Progress Environ. Sci. Technol.* **2009**, II (A, B), 289–292.

（14） You, X. J.; Liu, H.; Yang, G. Y.; Wang, Z. Y. *Chinese J. Struct. Chem.* **2009**, 28, 1311–1316.

（15） Liu, H.; Tan, J.; Yu, H. X.; Liu, H. X.; Wang, L. S.; Wang, Z. Y. *Int. J. Environ. Res.* **2010**, 4, 507–512.

（16） Waller, C. L. *J. Chem. Inf. Comput. Sci.* **2004**, 44, 758–765.

（17） Wang, H. Y.; Zhang, A. Q.; Sun, C.; Wang, L. S. *Chinese Sci. Bull.* **2008**, 53, 2292–2297.

（18） Frisch, M. J.; Trucks, G. W.; Schlegel, H. B.; Scuseria, G. E.; Robb, M. A.; Cheeseman, J. R.; Zakrzewski, V. G.; Montgomery, Jr. J. A.; Stratmann, R. E.; Burant, J. C.; Dapprich, S.; Millam, J. M.; Daniels, A. D.; Kudin, K. N.; Strain, M. C.; Farkas, O.; Tomasi, J.; Barone, V.; Cossi, M.; Cammi, R.; Mennucci, B.; Pomelli, C.; Adamo, C.; Clifford, S.; Ochterski, J.; Petersson, G. A.; Ayala, P. Y.; Cui, Q.; Morokuma, K.; Malick, D. K.; Rabuck, A. D.; Raghavachari, K.; Foresman, J. B.; Cioslowski, J.; Ortiz, J. V.; Baboul, A. G.; Stefanov, B. B.; Liu, G.; Liashenko, A.; Piskorz, P.; Komaromi, I.; Gomperts, R.; Martin, R. L.; Fox, D. J.; Keith, T.; Al-Laham, M. A.; Peng, C. Y.; Nanayakkara, A.; Challacombe, M.; Gill, P. M. W.; Johnson, B.; Chen, W.; Wong, M. W.; Andres, J. L.; Gonzalez, C.; Head-Gordon, M.; Replogle, E. S.; Pople, J. A. *Gaussian* 03, Revision A.1, Gaussian, Inc.: Pittsburgh **2003**.

（19） Ma, M.; Tong, Z. H.; Wang, Z. J. *J. Environ. Sci.* **1998**, 18, 86–90.

（20） Cramer, R. D.; Patterson, D. E.; Bunce, J. D. *J. Am. Chem. Soc.* **1988**, 110, 5959–5967.